Published in final edited form as:
Nat Chem Biol. 2010 July ; 6(7): 541–548. doi:10.1038/nchembio.385.

Structural basis of G protein-coupled receptor/G protein interactions

Jianxin Hu[1,*], **Yan Wang**[1], **Xiaohong Zhang**[1], **John R. Lloyd**[2], **Jianhua Li**[1], **Joel Karpiak**[3], **Stefano Costanzi**[3], and **Jürgen Wess**[1,*]

[1] Molecular Signaling Section, National Institutes of Health, Bethesda, Maryland 20892, USA

[2] Mass Spectrometry Group, Laboratory of Bioorganic Chemistry, National Institutes of Health, Bethesda, Maryland 20892, USA

[3] Laboratory of Biological Modeling, NIDDK, National Institutes of Health, Bethesda, Maryland 20892, USA

Abstract

The interaction of G protein-coupled receptors (GPCRs) with heterotrimeric G proteins represents one of the most fundamental biological processes. However, the molecular architecture of the GPCR/G protein complex remains poorly defined. In the present study, we applied a comprehensive GPCR/Gα chemical cross-linking strategy to map a receptor/Gα interface, both prior to and after agonist-induced receptor activation. By employing the M_3 muscarinic acetylcholine receptor (M3R)/$G\alpha_q$ system as a model system, we examined the ability of ~250 combinations of Cys-substituted M3R and $G\alpha_q$ proteins to undergo cross-link formation. We identified many specific M3R/$G\alpha_q$ contact sites, both in the inactive and the active receptor conformation, allowing us to draw conclusions regarding the basic architecture of the M3R/$G\alpha_q$ interface and the nature of the conformational changes following receptor activation. Since heterotrimeric G proteins as well as most GPCRs share a high degree of structural homology, our findings should be of broad general relevance.

INTRODUCTION

G protein-coupled receptors (GPCRs) are involved in regulating nearly all known physiological functions and represent excellent drug targets[1–3]. All GPCRs are predicted to contain a transmembrane (TM) core formed by a bundle of seven TM helices (TM1-7) which are connected by three extracellular and three intracellular loops (Fig. 1a). Physiologically, GPCRs are activated by extracellular ligands which enable the receptors to interact with and activate distinct sets of heterotrimeric G proteins (Gαβγ). Specifically, ligand-activated GPCRs catalyze the exchange of GDP for GTP on the Gα subunit. GTP

[*]Correspondence should be addressed to: Jürgen Wess, PhD Molecular Signaling Section, Laboratory of Bioorganic Chemistry, NIDDK, NIH, Bldg. 8A, Room B1A-05, 8 Center Drive MSC 0810, Bethesda, Maryland 20892, USA, Tel.: 301-402-3589, Fax: 301-480-3447, jwess@helix.nih.gov. Jianxin Hu, PhD, Molecular Signaling Section, Laboratory of Bioorganic Chemistry, NIDDK, NIH, Bldg. 8A, Room B1A-09, 8 Center Drive MSC 0810, Bethesda, Maryland 20892, USA, Tel: 301-594-5150, Fax: 301-480-3447, JianxinH@niddk.nih.gov.

Authors' Contributions

J.H. designed and conducted most of the biochemical experiments and wrote the paper. Y.W., X.Z., and J.L. were involved in the pharmacological characterization of the mutant proteins. J.R.L. carried out the mass spectrometry studies. S.C. carried out the molecular modeling studies and wrote the paper. J.K. performed modular modeling studies. J.W. designed the experiments and wrote the paper.

COMPETING INTERESTS STATEMENT

The authors declare no competing financial interests.

binding to Gα is predicted to trigger the dissociation of the heterotrimeric G protein into Gα-GTP and free βγ which are then able to modulate the activity of a multitude of downstream effector enzymes and ion channels[4].

High-resolution X-ray structures have been obtained for several class I GPCRs ('rhodopsin-like' GPCRs)[5–11] and various G protein heterotrimers (αβγ) and isolated Gα subunits in different functional states (for recent reviews, see refs. 12–14). Combined with biochemical and biophysical data[12–14], these structures reveal a surface on Gα that is predicted to face the intracellular side of GPCRs (see below for more details). However, a high-resolution crystal structure of a GPCR/G protein complex is not available at present.

Many studies have shown that multiple GPCR regions participate in receptor/G protein interactions[15]. These receptor regions include the TM3/i2 loop junction, the i2 loop, the cytoplasmic ends of TM5 and TM6, and helix 8 (H8; Fig 1a). Similarly, various experimental approaches have implicated multiple Gα regions in productive receptor/G protein coupling[12–14]. The three key regions of Gα that have been implicated by most studies include the N-terminal helix (αN; this helix is only observed in the presence of bound βγ), the α4/β6 loop, and the C-terminal portion[11–14,16–21].

Biochemical and biophysical approaches have identified a small number of receptor/Gα interaction sites using specific receptor/Gα combinations[11,19–21]. However, the molecular architecture of the receptor/Gα interface still remains poorly defined, primarily due to the lack of studies examining receptor/Gα contact sites in a systematic and comprehensive fashion. However, such knowledge is essential for understanding the structural basis underlying one of the most fundamental biological processes.

To address this question, we used the rat M_3 muscarinic acetylcholine receptor (M3R), a prototypic G_q-coupled receptor[22], as a model system. We carried out systematic cross-linking experiments using Cys-substituted M3R and $G\alpha_q$ constructs, both in the absence and presence of an activating ligand. To facilitate the interpretation of cross-linking data, we employed a modified version of the rat M3R lacking most native Cys residues (M3′(3C)-Xa; Fig. 1a)[23]. The M3′(3C)-Xa construct lacked the central portion of the third intracellular loop (i3 loop; A274–K469), resulting in the removal of three Cys residues contained within this region[23]. However, since this construct still retained the functionally critical N- and C-terminal portions of the i3 loop (Fig. 1a)[22], it can couple to G_q-type G protein with similar efficacy as the wild-type M3R[23]. Moreover, seven of the ten remaining endogenous M3R Cys residues were substituted with serine or alanine (Fig. 1a)[23]. A modified version of human $G\alpha_q$ ('$G\alpha_q$-C-less') in which we had replaced three of the five endogenous Cys residues with alanine served as a template for Cys substitution mutagenesis (Fig. 1b). In total, we examined cross-link formation between 18 mutant M3Rs and 14 mutant $G\alpha_q$ subunits (all constructs contained single Cys substitutions), in all possible combinations. These studies yielded many specific M3R/$G\alpha_q$ contact sites, both in the absence and presence of activating ligands, providing novel insights into the molecular architecture of the M3R/G_q interface and the potential mechanisms governing receptor-mediated G protein activation.

RESULTS

Generation of Cys-substituted mutant M3Rs

We introduced Cys substitutions into regions/sites of the M3′(3C)-Xa receptor known to be critical for M3R/G_q coupling (Fig. 1a)[22]. Recent studies carried out with several class I GPCRs strongly suggest that the cytoplasmic side of H8 is also critically involved in receptor/G protein interactions[15,24–27]. For this reason, we also targeted the corresponding

M3R residues (K548, T549, T552, T556, and L559) by Cys substitution mutagenesis (Fig. 1a).

Pharmacological properties of Cys-substituted mutant M3Rs

We first examined whether the various Cys-substituted mutant M3Rs retained the ability to bind muscarinic ligands with high affinity. Radioligand binding studies with membranes prepared from receptor-expressing COS-7 cells showed that all mutant M3Rs receptors were able to bind the muscarinic antagonist, [^{3}H]*N*-methylscopolamine ([^{3}H]NMS), with high affinity (range of [^{3}H]NMS K_D values: 163–877 pM; Supplementary Table 1). All mutant M3Rs were expressed at high density (range of [^{3}H]NMS B_{max} values: 5.4–16.4 pmol/mg), except for the D164C and Y166C receptors which were expressed at relatively low levels (B_{max}~ 1 pmol/mg; Supplementary Table 1). Moreover, [^{3}H]NMS/carbachol inhibition binding studies demonstrated that the different mutant M3Rs were able to bind the muscarinic agonist, carbachol, with affinities that were similar to or even higher than that observed with the M3′(3C)-Xa receptor from which all mutant receptors were derived (range of carbachol K_i values: 2.5–44.5 μM; Supplementary Table 1).

To examine whether the Cys-substituted mutant M3Rs retained the ability to couple to G_q-type G proteins, we studied their ability to mediate carbachol-induced increases in inositol phosphate (IP) production. Carbachol stimulation of receptor-expressing COS-7 cells led to pronounced increases in IP accumulation in all mutant receptors studied (Supplementary Table 1). However, several of the mutant receptors, including D164C, R165C, L173C, and Y254C, showed pronounced decreases in carbachol potency (increase in EC_{50}) and/or efficacy (decrease in E_{max}), as compared to the M3′ (3C)-Xa construct (Supplementary Table 1). This observation is consistent with the key roles of these residues in modulating the efficiency of receptor/G protein interactions[22].

Generation of Cys-substituted mutant $G\alpha_q$ proteins

Human $G\alpha_q$ contains five endogenous Cys residues which are located at positions 9, 10, 144, 219, and 330 (highlighted in yellow in Fig. 1b). We generated a mutant version of $G\alpha_q$ by replacing C144, C219, and C330 with alanine. In the following, we refer to this construct as '$G\alpha_q$-C-less'. This construct still contained two native Cys residues, C9 and C10, which proved to be essential for $G\alpha_q$ function (assessed in a second messenger assay; see below). In fact, it has been demonstrated that these two Cys residues are subject to palmitoylation which is required for proper G_q localization and function[28,29].

By using the $G\alpha_q$-C-less construct as a template, we introduced single Cys substitutions into $G\alpha_q$ domains that have been implicated in receptor/G protein interactions[12–18]. We first replaced the C-terminal five amino acids of $G\alpha_q$-C-less individually with Cys (E355C, Y356C, N357C, L358C, and V359C; Fig. 1b). Guided by a model of the G_q heterotrimer (see Methods for details), we also introduced single Cys residues into surface-exposed sites of the N-terminal domain (R19C, R20C, R27C, R30C, and R31C) and the α4/β6 loop (P318C, S320C, D321C, and K322C; Fig. 1b).

All mutant $G\alpha_q$ subunits retain functional activity

To study whether the various mutant $G\alpha_q$ constructs retained functional activity, we co-transfected HEK 293 cells with the different mutant $G\alpha_q$ constructs and a plasmid coding for the porcine α_{2A}-adrenergic receptor (α_{2A}-AR). Importantly, in this system, the α_{2A}-AR agonist, UK14304, triggers IP accumulation only in the presence of co-transfected $G\alpha_q$ (Supplementary Table 2)[30]. We found that all 14 Cys mutant $G\alpha_q$ constructs displayed robust functional activity in this assay system (Supplementary Table 2), indicating that the

various Cys substitutions did not disrupt receptor/G_q and $G\alpha_q$/effector (phospholipase Cβ) coupling.

General strategy used to identify M3R/$G\alpha_q$ contact sites

To detect specific M3R/$G\alpha_q$ contact sites, we co-expressed the 18 Cys mutant M3Rs with the 14 Cys mutant $G\alpha_q$ constructs, in all possible combinations (252 total). Subsequently, we exposed membranes prepared from co-transfected COS-7 cells to the oxidizing agent Cu(II)-(1,10-phenanthroline)$_3$ (CuPhen; 100 μM) to promote the formation of disulfide bonds between vicinal Cys residues. We monitored the successful formation of disulfide bonds by visualizing cross-linked receptor/G protein complexes via Western blotting carried out under non-reducing conditions. Since the $G\alpha_q$- and M3′(3C)-Xa-based constructs both have a molecular mass of ~40 kDa, the cross-linked receptor/$G\alpha_q$ complexes are predicted to have a size of ~80 kDa. All cross-linking reactions were carried out in the absence or presence of the muscarinic agonist, carbachol.

Cross-linking analysis of C-terminal mutant $G\alpha_q$ subunits

The five $G\alpha_q$ constructs containing C-terminal Cys substitutions (E355C, Y356C, N357C, L358C, and V359C) gave qualitatively similar cross-liking patterns (see next paragraph). The cross-linked receptor/$G\alpha_q$ complexes (~80 kDa in size) are indicated by arrows in Fig. 2a which shows cross-linking data obtained with a representative $G\alpha_q$ construct ($G\alpha_q$-L357C; for additional cross-linking data see Supplementary Figs. 1, 2). As expected, these bands could be detected by both anti-$G\alpha_q$ and anti-M3R antibodies (shown for the representative $G\alpha_q$-L357C/M3R-T556C combination in Fig. 2b). We did not observe any ~80 kDa bands when cells had been transfected with different mutant G protein or M3R constructs alone (Fig. 2b; also see Supplementary Fig. 3). These findings convincingly demonstrate that the ~80 kDa bands correspond to cross-linked receptor/$G\alpha_q$ complexes. Both the anti-$G\alpha_q$ and anti-M3R antibodies detected several additional immunoreactive bands which are likely to present non-crosslinked $G\alpha_q$ and M3R species as well as adducts with other proteins, consistent with the outcome of co-immunoprecipitation studies (see below).

All five $G\alpha_q$ subunits containing C-terminal Cys substitutions (E355C, Y356C, N357C, L358C, and V359C) could be cross-linked to multiple mutant M3Rs. These mutant M3Rs contained Cys substitutions in the i2 loop (L173C and R176C) and within the N-terminal portion of H8 (T549C, T552C, and T556C) (Fig. 2a; Supplementary Figs. 1, 3, and 4). All five mutant $G\alpha_q$ subunits cross-linked most efficiently with the T556C mutant M3R (Fig. 2a; Supplementary Fig. 1). All Cu-Phen-induced cross-links were confirmed by using the short, bi-functional, and irreversible chemical cross-linker, bis-maleimidoethane (BMOE; 0.5 mM), which can cross-link vicinal Cys residues (shown for a representative receptor/G protein combination, $G\alpha_q$-L358C/M3R-T556C, in Supplementary Fig. 3b).

Interestingly, essentially all cross-links observed in the absence of the muscarinic agonist, carbachol, were also detectable in the presence of this ligand (Fig. 2a; Supplementary Fig. 1). One possible explanation for this finding is that the M3R is pre-coupled to G_q prior to receptor activation, and that M3R activation by carbachol does not lead to the dissociation of the receptor/G_q complex due to the lack of GTP (or other guanine nucleotides) in the incubation buffer. Consistent with this concept, pretreatment of membrane preparations with GTPγS (100 μM), a hydrolytically stable GTP analog predicted to promote the dissociation of G protein heterotrimers and receptor/G protein complexes by displacing GDP from the Gα subunit, reduced the intensities of the observed receptor/$G\alpha_q$ cross-linking signals by ~40–70% (n=4; shown for the $G\alpha_q$-L357C/M3RT556C combination in Fig. 2b; also see Supplementary Fig. 3c).

To exclude the possibility that the cross-linking signals observed in the absence of carbachol were caused by agonist-independent receptor signaling (constitutive M3R activity), we carried out cross-linking studies in the presence of atropine (10 μM), an inverse muscarinic agonist[31,32]. We found that atropine treatment had no significant effect on the intensities of the observed disulfide cross-linking signals (shown for the $G\alpha_q$-L357C/M3R-T556C combination in Fig. 2b; also see Supplementary Fig. 3c), suggesting that the cross-linking pattern obtained in the absence of carbachol reflects the structure of the inactive M3R/G_q complex.

Although most cross-links involving the C-terminus of $G\alpha_q$ occurred with similar efficiency in the absence or presence of carbachol, we noted that carbachol treatment greatly enhanced the efficiency of disulfide cross-linking in several cases. We found that carbachol strongly promoted cross-linking between the A488C mutant M3R and the last three amino acids of $G\alpha_q$ (N357C, L358C, and V359C; Fig. 2c). Agonist treatment also led to slightly stronger cross-linking signals between the T549C and T552C mutant M3Rs and several $G\alpha_q$ subunits containing C-terminal Cys substitutions (Supplementary Fig. 4).

Co-immunoprecipitation and mass spectrometry studies

To further confirm that the ~80 kDa immunoreactive species observed in the cross-linking experiments do in fact represent $G\alpha_q$/M3R complexes, we carried out a series of co-immunoprecipitation experiments. Specifically, we studied the representative N357C-$G\alpha_q$/T556C-M3R pair and two other receptor/G protein combinations described in more detail below (R31C-$G\alpha_q$/L173C-M3R, and D321C-$G\alpha_q$/K548C-M3R. Initially, we incubated membrane proteins prepared from COS-7 cells that had been co-transfected with the three different receptor/G protein pairs with either 100 μM Cu-Phen (N357CG α_q/T556C-M3R and R31C-$G\alpha_q$/L173C-M3R) or 0.5 mM BMOE (D321C-$G\alpha_q$/K548C-M3R) to induce cross-link formation. Following membrane lysis, we immunoprecipitated M3R-containing proteins with a polyclonal anti-M3 antibody, followed by Western blotting studies using an anti-$G\alpha_q$ monoclonal antibody. In a reciprocal fashion, we immunoprecipitated $G\alpha_q$-containing proteins with the anti-$G\alpha_q$ antibody, followed by Western blotting studies using the anti-M3R antibody. In all co-immunoprecipitation experiments, the ~80 kDa band was the only immunoreactive species that was consistently detectable by both the anti-M3 and anti-$G\alpha_q$ antibodies (shown for the representative N357C-$G\alpha_q$/T556C-M3R combination in Fig. 3; for additional co-immunoprecipitation data, see Supplementary Fig. 5). We did not observe this band using samples derived from cells that had been transfected with the individual receptor or G protein constructs alone (Fig. 3; Supplementary Fig. 5). These findings strongly support the notion that the ~80 kDa immunoreactive bands observed in the cross-linking experiments correspond to cross-linked receptor/$G\alpha_q$ complexes.

We also confirmed the structural identity of a putative $G\alpha_q$/M3R complex (N357C-$G\alpha_q$/T556C-M3R) via LC/MS/MS analysis (see Supplementary Results and Supplementary Fig. 6 for details).

A cross-link between αN of $G\alpha_q$ and the i2 loop of the M3R

To identify potential contact sites between the αN helix of $G\alpha_q$ (in the G_q heterotrimer) and the intracellular surface of the M3R, we examined Cu-Phen-dependent cross-link formation between the R19C, R20C, R27C, R30C, and R31C mutant $G\alpha_q$ subunits (Fig. 1b) and the 18 Cys-substituted mutant M3Rs (Fig. 1a). Four of the five G protein constructs (R19C, R20C, R27C, and R30C) failed to display any significant cross-linking with any of the analyzed mutant M3Rs, independent of the absence or presence of carbachol (Supplementary Fig. 7). However, we observed a clear cross-linking signal between the R31C-$G\alpha_q$ subunit and the L173C receptor (Fig. 4). As expected, the band corresponding to the cross-linked R31C-

$G\alpha_q$/L173C-M3R complex could be detected by both anti-$G\alpha_q$ and anti-M3R antibodies (Fig. 4b; Supplementary Fig. 8). Moreover, this $G\alpha_q$/M3R adduct was not observed when cells had been transfected with the R31C-$G\alpha_q$ or L173C-M3R constructs alone (Fig. 4b; Supplementary Fig. 8), providing further evidence for the specificity of the observed interaction (for detection of the R31C-$G\alpha_q$/L173C-M3R complex in co-immunoprecipitation studies, see Supplementary Fig. 5a, b). The intensity of the R31C-$G\alpha_q$/L173C-M3R cross-linking signal remained essentially unaffected by the addition of the agonist, carbachol (1 mM; Fig. 4a; Supplementary Fig. 8), or the inverse agonist, atropine (10 μM; Fig. 4b), but was significantly reduced by pretreatment of membranes with GTPγS (100 μM; Fig. 4b).

An agonist-induced α4/β6 loop ($G\alpha_q$)/H8 (M3R) cross-link

To elucidate potential points of interactions between the α4/β6 loop of $G\alpha_q$ and the cytoplasmic side of the M3R, we studied cross-link formation between the P318C, S320C, D321C, and K322C mutant $G\alpha_q$ subunits (Fig. 1b) and the 18 Cys-substituted mutant M3Rs (Fig. 1a). Since it proved difficult to detect K322C-$G\alpha_q$ via Western blotting, we excluded this construct from further studies. By using Cu-Phen as an oxidizing agent, we were unable to detect any significant, reproducible cross-links between the P318C, S320C, and D321C $G\alpha_q$ constructs and any of the 18 mutant M3Rs (Supplementary Fig. 9), independent of the absence or presence of carbachol (1 mM). We therefore carried out additional cross-linking studies with the bifunctional, irreversible chemical cross-linking reagent, BMOE. Independent of the absence or presence of carbachol, BMOE (0.5 mM) treatment failed to induce any significant, reproducible cross-links between most mutant $G\alpha_q$ (P318C, S320C, or D321C)/M3R combinations (Fig. 5a; Supplementary Fig. 10). However, in the absence of carbachol, incubation with BMOE (0.5 mM) led to faint cross-linking signals between the D321C-$G\alpha_q$ subunit and three mutant M3Rs containing Cys substitutions within the N-terminal segment of H8 (K548C, T549C, and T552C; Fig. 5a, b). Strikingly, in all three cases, carbachol treatment greatly enhanced the intensities of the cross-linked adducts (Fig. 5a, b), consistent with the outcome of co-immunoprecipitation studies (shown for the representative D321C-$G\alpha_q$/K548C-M3R complex in Supplementary Fig. 5c, d). These agonist-induced increases in cross-linking efficiency could be abolished or greatly reduced by pretreatment of membranes with GTPγS (100 μM) or atropine (10 μM) (shown for the representative D321C-$G\alpha_q$/K548C-M3R combination in Fig. 5b).

Cell surface expression of cross-linked M3R/$G\alpha_q$ pairs

To confirm that the cross-linked Cys-substituted M3R/$G\alpha_q$ pairs were present on the cell surface, we incubated intact COS-7 cells expressing different M3R/$G\alpha_q$ combinations with the membrane-impermeable biotinylation reagent, sulfo-NHS-S-S-biotin (see Supplementary Methods for details). After treatment of cell membranes with BMOE (0.5 mM) and membrane lysis, we isolated biotinylated cell surface proteins by using agarose-conjugated streptavidin. We then analyzed biotinylated proteins via Western blotting. These studies confirmed the presence of biotinylated M3R/$G\alpha_q$ complexes, indicating that M3R/$G\alpha_q$ cross-linking occurred at the cell surface (shown for the representative N357C-$G\alpha_q$/T556C-M3R and D321C-$G\alpha_q$/K548C-M3R combinations in Supplementary Fig. 11).

Effect of receptor densities on $G\alpha_q$/M3R cross-linking

In the present study, many of the modified M3Rs were expressed at rather high levels (>10 pmol/mg). To examine whether the observed cross-linking patterns could also be observed at lower (more physiological) receptor levels, we drastically reduced the expression levels 17 of three key mutant M3Rs (T556C, L173C, and D321C) to ~1 pmol/mg (by reducing the amount of transfected receptor DNA; see Methods for details). Following co-expression with N357C-$G\alpha_q$ (T556C-M3R), R31C-$G\alpha_q$ (L173C-M3R), or D321C-$G\alpha_q$(K548C-M3R), respectively, the resulting cross-linking patterns were qualitatively similar to those obtained

when the mutant receptors were expressed at considerably higher levels (Supplementary Fig. 12). The N357C-$G\alpha_q$/T556C-M3R and R31C-$G\alpha_q$/L173C-M3R combinations showed basal disulfide cross-linking that was not affected by the presence of carbachol, whereas the D321C-$G\alpha_q$/K548C-M3R pair displayed pronounced agonist-inducible disulfide cross-linking (Supplementary Fig. 12).

To compare the expression levels of $G\alpha_q$ endogenously expressed in COS-7 cells with those of the transiently expressed modified $G\alpha_q$ subunits, we determined the intensities of immunoreactive $G\alpha_q$ bands via scanning densitometry. This analysis showed that endogenous $G\alpha_q$ and the mutationally modified $G\alpha_q$ subunits were expressed at approximately similar levels (arbitrary units: endogenous $G\alpha_q$, 100; mutant $G\alpha_q$ subunits; 140 ± 18; n=18). Taken together, these findings indicate that it is highly likely that the observed disulfide cross-linking patterns are physiologically relevant.

Discussion

In the present study, we observed several M3R/$G\alpha_q$ cross-links even in the absence of activating ligands. These cross-links were not affected by treatment of samples with the inverse muscarinic agonist, atropine[31,32], suggesting that they were not caused by agonist-independent M3R signaling but most likely reflect the existence of preformed M3R/$G\alpha_q$ complexes[33–37]. One of these agonist-independent cross-links occurred between a residue located on the surface-exposed side of the αN helix of $G\alpha_q$ (R31C) and a residue located in the i2 loop of the M3R (L173C). Interestingly, most class I GPCRs contain a leucine residue or another relatively bulky lipophilic amino acid at the position corresponding to L173 in the M3R[38,39]. Site-directed mutagenesis studies with different GPCRs have shown that the presence of this residue is critical for productive receptor/G proteins interactions (see, for example, refs. 38, 39; also see Supplementary Table 1). Our cross-linking data therefore support the novel concept that direct contacts between the i2 loop of the receptor and the αN helix of Gα play a central role in productive receptor/G protein coupling.

Most M3R/$G\alpha_q$ contact sites identified in the inactive state of the M3R were also observed following activation of the M3R by carbachol. The most likely explanation for this finding is that the M3R is precoupled to G_q prior to receptor activation, and that carbachol-mediated M3R activation does not result in the dissociation of the receptor/G_q complex due to the lack of GTP (or other guanine nucleotides) in the incubation buffer. The M3R/$G\alpha_q$ cross-linking signals that we detected in the presence of carbachol therefore most likely reflect the structural organization of the M3R/G_q complex in which the guanine nucleotide binding pocket of the G_q heterotrimer is ‘empty’. It is well known that 19 heterotrimeric G proteins with an empty nucleotide binding pocket interact with GPCRs with very high affinity[40].

We also detected several cross-links that showed very strong agonist dependence. Most strikingly, we identified a carbachol-induced cross-link between a residue located in the α4/β6 loop of $G\alpha_q$ (D321C) and the N-terminal segment of H8 of the M3R (K548C, T549C, and T552C). This finding suggests that receptor activation leads to a structural change at the receptor/G_q interface that increases the proximity between the N-terminal portion of H8 of the M3R and the α4/β6 loop of $G\alpha_q$. The agonist carbachol also promoted significant cross-linking between a residue located at the cytoplasmic end of TM6 of the M3R (A488C) and the last three residues of $G\alpha_q$ (N357C, L358C, and V359C). Since M3R residue A488 (residue 6.33 according to the Ballesteros-Weinstein GPCR numbering system)[41] is predicted to be buried in the TM core in the inactive conformation of the receptor[5–8], this observation supports previous findings that GPCR activation involves an opening of the intracellular receptor surface, allowing the C-terminus of Gα to make productive interactions with previously buried TM5 and TM6 residues of the receptor[11,42,43]. Agonist treatment

also led to more intense cross-linking signals between the N-terminal portion of H8 of the M3R (T549C and T552C) and the C-terminus of $G\alpha_q$, indicating that these regions move closer to each other following M3R activation. However, we cannot completely exclude the possibility that the promiscuous cross-linking pattern observed with the mutant $G\alpha_q$ subunits containing C-terminal Cys substitutions is caused by the existence of multiple conformational states of the receptor/G protein complex.

It is likely that these agonist-promoted conformational changes at the M3R/$G\alpha_q$ interface play a key role in receptor-catalyzed GDP release from G_q. The C-terminus of Gα is linked to the β6/α5 loop of Gα via the α5 helix (note that the β6/α5 loop contains residues that are critical for guanine nucleotide binding). Interestingly, a recent biophysical study suggests that a rotational/translation movement of the α5 helix is critical for receptor (rhodopsin)-mediated GDP release from the G protein[44]. Analogously, the agonist-induced contact between H8 of the M3R and the α4/β6 loop of $G\alpha_q$ observed in the present study may alter the orientation of the β6/α5 loop by conformational changes that are propagated from the α4/β6 loop to the adjacent β6 strand (also see refs. 21 and 45).

The observed M3R/$G\alpha_q$ cross-linking patterns provided many structural constraints that allowed us to generate a model of the M3R/$G\alpha_q\beta\gamma$ complex in its inactive state (Fig. 6) (see Supplementary Methods and Supplementary Table 3 for details). A key feature of this model is that the αN helix of $G\alpha_q$ is located adjacent to the i2 loop of the M3R. The highly flexible C-terminal portion of $G\alpha_q$ points diagonally towards the intracellular opening of the M3R, where it can make contacts with residues located on the i2 loop and H8. Moreover, the N-terminus of $G\alpha_q$ and the C-terminus of Gγ, both of which carry lipid modifications, are in proximity of the plasma membrane. The agonist-promoted cross-links between the extreme C-terminus of $G\alpha_q$ and position A488 of the M3R (bottom of TM6) and between the α4/β6 loop of $G\alpha_q$ and H8 support a model in which agonist-induced conformational changes on the intracellular receptor surface allow Gα (including the α4/β6 loop) to move closer towards and interact more extensively with the receptor (indicated by arrows in Fig. 6).

In the present study, we focused on identifying receptor contact sites for three key regions of $G\alpha_q$ known to be critically involved in receptor/G protein interactions. However, it should be noted that several other Gα regions as well as sites on the G protein βγ complex have also been implicated in receptor/G protein coupling[12–14].

The M3R/$G\alpha_q$ cross-linking patterns observed in the present study can be explained by the interaction of one M3R monomer with one $G\alpha_q$ subunit. However, our data do not rule out the existence of M3R dimers or oligomers[46,47].

In summary, the present study represents the first analysis examining receptor/Gα interaction sites in a systematic and comprehensive fashion. Importantly, all experimental data were obtained with functional receptor and Gα proteins present in a native membrane environment (*in situ*). Since heterotrimeric G proteins as well as most GPCRs share a high degree of structural homology, our findings should be of broad general relevance.

METHODS

Materials

Carbamylcholine chloride (carbachol), atropine sulfate, cupric sulfate ($CuSO_4$), UK14304, 1,10-phenanthroline, and *N*-ethylmaleimide were purchased from Sigma. BMOE and sulfo-NHS-S-S-biotin were from Thermo Scientific. [^{3}H]NMS (70.0 Ci/mmol) and *myo*-[^{3}H]inositol (20 Ci/mmol) were obtained from PerkinElmer Life Sciences. $CuSO_4$ was mixed with 1,10-phenanthroline at a molar ratio of 1:3 (ref. 32). The concentrations

indicated in the text for the Cu(II)-(1,10-phenanthroline)$_3$ complex (Cu-Phen) refer to molar copper concentrations.

Construction of Cys-substituted mutant M3R and Gα$_q$ constructs

All receptor Cys substitutions were introduced into a pCD-based expression plasmid coding for a modified version of the rat M3R referred to as M3′(3C)-Xa (Fig. 1a)[23]. This receptor construct lacks most endogenous Cys residues, except for C140, C220, and C532 which proved to be essential for M3R function, all five *N*-glycosylation sites contained within the extracellular N-terminal domain, as well as the central portion of the i3 loop (A274–K469; this region was replaced with two adjacent factor Xa cleavage sites)[23]. Cys residues were substituted into the M3′ (3C)-Xa construct by using the QuikChange™ site-directed mutagenesis kit (Stratagene) according to the manufacturer's instructions. Using a similar strategy, we generated a mutant version of human Gα$_q$ (in the pcDNA3.1 vector), termed Gα$_q$-C-less, in which three of the five native Cys residues were replaced with alanine (C144, C219, and C330; Fig. 1b). All Cys substitutions were introduced into the Gα$_q$-C-less construct. The identity of all mutant M3R and Gα$_q$ constructs was confirmed by sequencing the entire coding sequences.

Transient expression of Cys-substituted mutant M3R and Gα$_q$ constructs in cultured cells

For radioligand binding and functional studies, all receptor constructs were transiently expressed in COS-7 cells, as described previously[32]. To increase receptor expression levels, transfected cells were incubated with 1 μM atropine for the last 24 h of culture. For disulfide cross-linking experiments, COS-7 cells were co-transfected with receptor and Gα$_q$ plasmid DNAs (2.5 μg each per 100 mm dish), using conditions similar to those described previously[32]. To lower the expression levels for selected mutant M3Rs, COS-7 cells were co-transfected with 0.05 μg of receptor DNA, 2.45 μg vector DNA, and 2.5 μg Gα$_q$ DNA (per 100 mm dish). To examine whether the various mutant Gα$_q$ constructs retained functional activity, we transiently co-expressed the different mutant Gα$_q$ constructs with a pCMV4-based plasmid coding for the porcine α$_{2A}$-adrenergic receptor (α$_{2A}$-AR)[30]. Specifically, 3×10^5 HEK 293 cells were seeded into 25 cm^2 flasks 24 h prior to transfections. Cells were co-transfected with 1 μg of the α$_{2A}$-AR construct and 3 μg of mutant Gα$_q$ DNA. About 24 h later, transfected cells were split into 12-well plates for PI hydrolysis assays.

Preparation of membranes from transfected COS-7 cells

COS-7 cells were harvested ~48 h after transfections, and membranes were prepared for radioligand binding and disulfide cross-linking studies as described[32].

Radioligand binding studies

The various mutant M3Rs were characterized in [^{3}H]NMS saturation and in [^{3}H]NMS/carbachol competition binding assays. Binding studies were carried out using membranes prepared from transfected COS-7 cells, as described in detail previously[32].

Measurement of receptor-mediated PI hydrolysis

To examine whether the various mutant M3Rs retained the ability to activate G proteins, we determined carbachol-mediated increases in intracellular inositol monophosphate (IP) levels. PI assays were carried out essentially as described[32]. To verify that the different mutant Gα$_q$ subunits retained functional activity, we also performed PI assays with HEK 293 cells co-transfected with the porcine α$_{2A}$-AR and the different Gα$_q$ mutant constructs. Transfected HEK-293 cells grown in 12-well plates were incubated with 3 μCi/ml myo-[^{3}H]inositol for the last 24 h of culture. We then determined the ability of the α$_{2A}$-AR agonist, UK14304, to

stimulate increases in intracellular IP levels[32]. PI data were analyzed using the nonlinear curve-fitting program Prism 4.0 (GraphPad).

Disulfide cross-linking and solubilization of Cys-substituted $G\alpha_q$ and M3R proteins

Disulfide cross-linking studies were carried out as described in detail previously[32]. In brief, receptor/$G\alpha_q$-containing membranes prepared from co-transfected COS-7 cells were incubated either with the oxidizing agent, Cu-Phen (100 μM), or with the irreversible chemical cross-linker, BMOE (0.5 mM), in the absence or presence of 1 mM carbachol. Reactions were carried out for 10 min at 22 °C and then terminated by the addition of either EDTA and *N*-ethylmaleimide (10 mM each; Cu-Phen-induced cross-linking) or 10 mM DTT (BMOE-mediated cross-linking), followed by a 10-min incubation on ice. Subsequently, membrane proteins were solubilized by incubating samples with 1.2% digitonin (Roche Applied Science)[32]. Samples were then stored at −70 °C or used directly for SDS-PAGE.

Western blot analysis

SDS-PAGE and Western blotting studies were carried out as described previously[32]. In brief, samples containing 20 μg of solubilized membrane protein were incubated with Laemmli loading buffer for 30 min at 37 °C, either under nonreducing (Cu-Phen-induced cross-linking) or under reducing conditions (BMOE-mediated cross-linking), in the absence or presence of 10% β-mercaptoethanol, respectively. Blots were first probed with an anti-$G\alpha_q$ monoclonal antibody directed against residues 22–31 of human $G\alpha_q$ (BD Biosciences), followed by incubation with secondary goat anti-mouse HRP conjugate (Calbiochem). This antibody failed to detect the R27C and R30C mutant $G\alpha_q$ subunits with high efficiency (note that R27 and R30 are contained within the antibody recognition sequence). However, we were able to detect these two mutant G protein constructs using a rabbit polyclonal anti-$G\alpha_q$ antibody directed against the C-terminal domain (residues 350–359) of mammalian $G\alpha_{q/11}$ (Calbiochem). All $G\alpha_q$ blots were routinely stripped by using OneMinute Western Blot Stripping Buffer (GM Biosciences) and reprobed with a rabbit anti-M3R polyclonal antibody directed against the C-terminal 18 amino acids of the rat M3R[32]. Immunoreactive proteins were visualized by using SuperSignal West Pico Chemiluminescent Substrate (Pierce) and autoradiography[32].

Construction of homology models and docking of G_q to the M3R

The procedures used for constructing a molecular model of the M3R/G_q complex are described in detail under Supplementary Methods. The model that was most compatible with the observed cross-linking data is shown in Fig. 6 (see text for details). The coordinates on which this model is based are provided as a pdb file (M3R_Gq.pdb) under Supplementary Information.

Data analysis

Data were presented as mean ± s. e. m. for the indicated number of experiments. Sigmoidal concentration-response data were analyzed using the nonlinear curve-fitting program Prism 4.0 (GraphPad). Statistical significance was determined using the Student's t-test.

Supplementary Material

Refer to Web version on PubMed Central for supplementary material.

Acknowledgments

This research was supported by the Intramural Research Program of the NIDDK, NIH, and utilized the high-performance computational capabilities of the Biowulf Linux cluster at the NIH, Bethesda, MD (http://biowulf.nih.gov).

References

1. Pierce KL, Premont RT, Lefkowitz RJ. Seven-transmembrane receptors. Nat Rev Mol Cell Biol. 2002; 3:639–650. [PubMed: 12209124]
2. Lagerström MC, Schiöth HB. Structural diversity of G protein-coupled receptors and significance for drug discovery. Nat Rev Drug Discov. 2008; 7:339–357. [PubMed: 18382464]
3. Regard JB, Sato IT, Coughlin SR. Anatomical profiling of G protein-coupled receptor expression. Cell. 2008; 135:561–571. [PubMed: 18984166]
4. Cabrera-Vera TM, et al. Insights into G protein structure, function, and regulation. Endocr Rev. 2003; 24:765–781. [PubMed: 14671004]
5. Palczewski K, et al. Crystal structure of rhodopsin: A G protein-coupled receptor. Science. 2000; 289:739–745. [PubMed: 10926528]
6. Warne T, et al. Structure of a β_1-adrenergic G-protein-coupled receptor. Nature. 2008; 454:486–491. [PubMed: 18594507]
7. Cherezov V, et al. High-resolution crystal structure of an engineered human β_2-adrenergic G protein-coupled receptor. Science. 2007; 318:1258–1265. [PubMed: 17962520]
8. Rasmussen SG, et al. Crystal structure of the human β_2 adrenergic G-protein-coupled receptor. Nature. 2007; 450:383–387. [PubMed: 17952055]
9. Jaakola VP, et al. The 2.6 angstrom crystal structure of a human A_{2A} adenosine receptor bound to an antagonist. Science. 2008; 322:1211–1217. [PubMed: 18832607]
10. Park JH, Scheerer P, Hofmann KP, Choe HW, Ernst OP. Crystal structure of the ligand-free G-protein-coupled receptor opsin. Nature. 2008; 454:183–187. [PubMed: 18563085]
11. Scheerer P, et al. Crystal structure of opsin in its G-protein-interacting conformation. Nature. 2008; 455:497–502. [PubMed: 18818650]
12. Oldham WM, Hamm HE. How do receptors activate G proteins? Adv Protein Chem. 2007; 74:67–93. [PubMed: 17854655]
13. Oldham WM, Hamm HE. Heterotrimeric G protein activation by G-protein-coupled receptors. Nat Rev Mol Cell Biol. 2008; 9:60–71. [PubMed: 18043707]
14. Johnston CA, Siderovski DP. Receptor-mediated activation of heterotrimeric G-proteins: current structural insights. Mol Pharmacol. 2007; 72:219–230. [PubMed: 17430994]
15. Wess J. Molecular basis of receptor/G-protein-coupling selectivity. Pharmacol Ther. 1998; 80:231–264. [PubMed: 9888696]
16. Hamm HE, et al. Site of G protein binding to rhodopsin mapped with synthetic peptides from the α subunit. Science. 1988; 241:832–835. [PubMed: 3136547]
17. Onrust R, et al. Receptor and βγ binding sites in the α subunit of the retinal G protein transducin. Science. 1997; 275:381–384. [PubMed: 8994033]
18. Conklin BR, Farfel Z, Lustig KD, Julius D, Bourne HR. Substitution of three amino acids switches receptor specificity of $G_q\alpha$ to that of $G_i\alpha$. Nature. 1993; 363:274–276. [PubMed: 8387644]
19. Cai K, Itoh Y, Khorana HG. Mapping of contact sites in complex formation between transducin and light-activated rhodopsin by covalent crosslinking: use of a photoactivatable reagent. Proc Natl Acad Sci USA. 2001; 98:4877–4882. [PubMed: 11320237]
20. Itoh Y, Cai K, Khorana HG. Mapping of contact sites in complex formation between light-activated rhodopsin and transducin by covalent crosslinking: use of a chemically preactivated reagent. Proc Natl Acad Sci USA. 2001; 98:4883–4887. [PubMed: 11320238]
21. Johnston CA, Siderovski DP. Structural basis for nucleotide exchange on $G\alpha_i$ subunits and receptor coupling specificity. Proc Natl Acad Sci USA. 2007; 104:2001–2006. [PubMed: 17264214]

22. Wess J. Molecular biology of muscarinic acetylcholine receptors. Crit Rev Neurobiol. 1996; 10:69–99. [PubMed: 8853955]
23. Zeng FY, Hopp A, Soldner A, Wess J. Use of a disulfide cross-linking strategy to study muscarinic receptor structure and mechanisms of activation. J Biol Chem. 1999; 274:16629–16640. [PubMed: 10347230]
24. Cai K, et al. Single-cysteine substitution mutants at amino acid positions 306–321 in rhodopsin, the sequence between the cytoplasmic end of helix VII and the palmitoylation sites: sulfhydryl reactivity and transducin activation reveal a tertiary structure. Biochemistry. 1999; 38:7925–7930. [PubMed: 10387034]
25. Ernst OP, et al. Mutation of the fourth cytoplasmic loop of rhodopsin affects binding of transducin and peptides derived from the carboxyl-terminal sequences of transducin α and γ subunits. J Biol Chem. 2000; 275:1937–1943. [PubMed: 10636895]
26. Swift S, et al. Role of the PAR1 receptor 8th helix in signaling: the 7-8-1 receptor activation mechanism. J Biol Chem. 2006; 281:4109–4116. [PubMed: 16354660]
27. Delos Santos NM, Gardner LA, White SW, Bahouth SW. Characterization of the residues in helix 8 of the human β_1-adrenergic receptor that are involved in coupling the receptor to G proteins. J Biol Chem. 2006; 281:12896–12907. [PubMed: 16500896]
28. Wedegaertner PB, Chu DH, Wilson PT, Levis MJ, Bourne HR. Palmitoylation is required for signaling functions and membrane attachment of $G_q\alpha$ and $G_s\alpha$. J Biol Chem. 1993; 268:25001–25008. [PubMed: 8227063]
29. Edgerton MD, Chabert C, Chollet A, Arkinstall S. Palmitoylation but not the extreme amino-terminus of $G_{q\alpha}$ is required for coupling to the NK2 receptor. FEBS Lett. 1994; 354:195–199. [PubMed: 7957923]
30. Chabre O, Conklin BR, Brandon S, Bourne HR, Limbird LE. Coupling of the α_{2A}-adrenergic receptor to multiple G-proteins. A simple approach for estimating receptor-G-protein coupling efficiency in a transient expression system. J Biol Chem. 1994; 269:5730–5734. [PubMed: 7907086]
31. Spalding TA, Burstein ES, Brauner-Osborne H, Hill-Eubanks D, Brann MR. Pharmacology of a constitutively active muscarinic receptor generated by random mutagenesis. J Pharmacol Exp Ther. 1995; 275:1274–1279. [PubMed: 8531092]
32. Li JH, et al. Distinct structural changes in a G protein-coupled receptor caused by different classes of agonist ligands. J Biol Chem. 2007; 282:26284–93. [PubMed: 17623649]
33. Rebois RV, Hébert TE. Protein complexes involved in heptahelical receptor-mediated signal transduction. Receptors Channels. 2003; 9:169–194. [PubMed: 12775338]
34. Nobles M, Benians A, Tinker A. Heterotrimeric G proteins precouple with G protein-coupled receptors in living cells. Proc Natl Acad Sci USA. 2005; 102:18706–18711. [PubMed: 16352729]
35. Galés C, et al. Real-time monitoring of receptor and G-protein interactions in living cells. Nat Methods. 2005; 2:177–184. [PubMed: 15782186]
36. Clark MA, Sethi PR, Lambert NA. Active $G\alpha_q$ subunits and M3 acetylcholine receptors promote distinct modes of association of RGS2 with the plasma membrane. FEBS Lett. 2007; 581:764–770. [PubMed: 17275815]
37. Lohse MJ, et al. Optical techniques to analyze real-time activation and signaling of G-protein-coupled receptors. Trends Pharmacol Sci. 2008; 29:159–165. [PubMed: 18262662]
38. Moro O, Lameh J, Högger P, Sadée W. Hydrophobic amino acid in the i2 loop plays a key role in receptor-G protein coupling. J Biol Chem. 1993; 268:22273–22276. [PubMed: 8226735]
39. Wacker JL, et al. Disease-causing mutation in GPR54 reveals the importance of the second intracellular loop for class A G-protein-coupled receptor function. J Biol Chem. 2008; 283:31068–310678. [PubMed: 18772143]
40. Bornancin F, Pfister C, Chabre M. The transitory complex between photoexcited rhodopsin and transducin. Eur J Biochem. 1989; 184:687–98. [PubMed: 2509200]
41. Ballesteros JA, Weinstein H. Integrated methods for modeling G-protein coupled receptors. Meth Neurosci. 1995; 25:366–428.

42. Hubbell WL, Altenbach C, Hubbell CM, Khorana HG. Rhodopsin structure, dynamics, and activation: a perspective from crystallography, site-directed spin labeling, sulfhydryl reactivity, and disulfide cross-linking. Adv Protein Chem. 2003; 63:243–290. [PubMed: 12629973]

43. Altenbach C, Kusnetzow AK, Ernst OP, Hofmann KP, Hubbell WL. High-resolution distance mapping in rhodopsin reveals the pattern of helix movement due to activation. Proc Natl Acad Sci USA. 2008; 105:7439–7444. [PubMed: 18490656]

44. Oldham WM, Van Eps N, Preininger AM, Hubbell WL, Hamm HE. Mechanism of the receptor-catalyzed activation of heterotrimeric G proteins. Nat Struct Mol Biol. 2006; 13:772–777. [PubMed: 16892066]

45. Kapoor N, Menon ST, Chauhan R, Sachdev P, Sakmar TP. Structural evidence for a sequential release mechanism for activation of heterotrimeric G proteins. J Mol Biol. 2009; 393:882–897. [PubMed: 19703466]

46. Javitch JA. The ants go marching two by two: oligomeric structure of G-protein-coupled receptors. Mol Pharmacol. 2004; 66:1077–1082. [PubMed: 15319448]

47. Milligan G, Bouvier M. Methods to monitor the quaternary structure of G protein-coupled receptors. FEBS J. 2005; 272:2914–2925. [PubMed: 15955052]

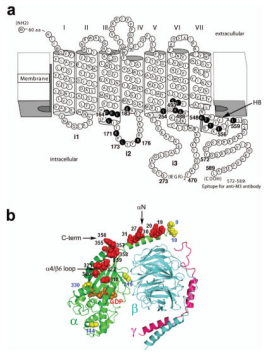

Figure 1.

Introduction of Cys substitutions into the M3R and $G\alpha_q$. (**a**) Secondary structure of a modified version of the rat M3R (M3′(3C)-Xa). All Cys substitutions were introduced into the M3′ (3C)-Xa construct[23] that lacked most endogenous Cys residues and the central portion of the i3 loop (A274–K469; see Methods for details). Endogenous Cys residues were substituted with serine or alanine (open squares), except for C140, C220 and C532 which proved to be essential for proper receptor function[23]. Amino acids that were replaced with Cys residues are highlighted by black circles. The numbering of M3R residues is based on the sequence of the full-length rat M3R. **(b)** Model of human $G\alpha_q$ (green) in complex with a βγ dimer (β, cyan; γ, purple). The five endogenous Cys residues present in $G\alpha_q$ are highlighted in yellow. We introduced Cys substitutions into a modified version of $G\alpha_q$ ($G\alpha_q$-C-less) in which C144, C219, and C330 had been replaced with alanine (C9 and C10 were found to be critical for $G\alpha_q$ function and were therefore left intact). Amino acids in $G\alpha_q$ that were subjected to Cys substitution mutagenesis are highlighted in red. The model of the G_q trimer was generated as described under Methods.

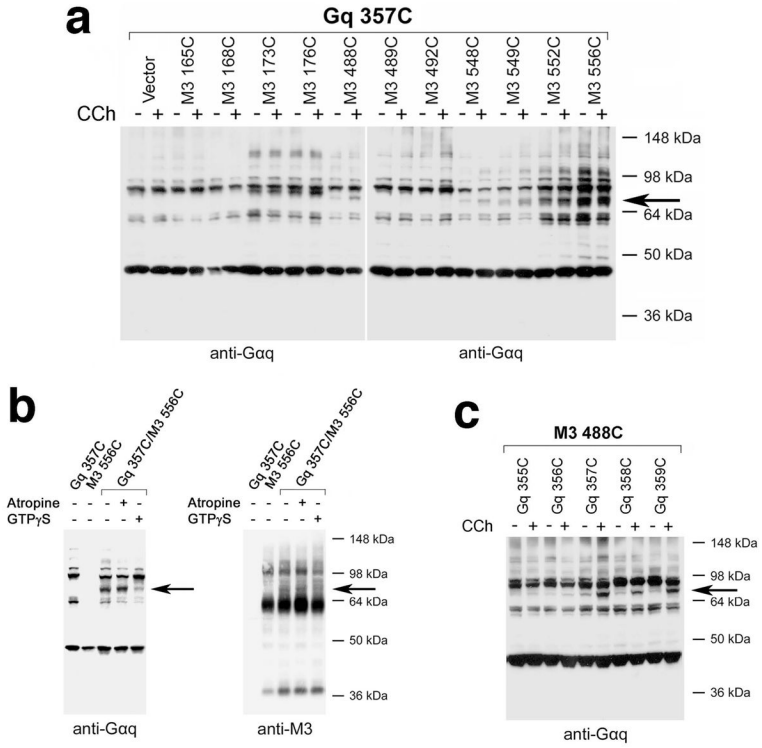

Figure 2.

Cross-linking of $G\alpha_q$ subunits containing C-terminal Cys substitutions with Cyssubstituted mutant M3Rs. (**a**) Cross-link formation between the N357C $G\alpha_q$ construct and selected mutant M3Rs. (**b**) Effect of atropine and GTPγS treatment on cross-link formation between N357C-$G\alpha_q$ and the T556C mutant M3R. (**c**) Agonist-promoted cross-link formation between $G\alpha_q$ subunits containing C-terminal Cys substitutions and the A488C mutant M3R. To induce cross-link formation, membrane proteins prepared from transfected COS-7 cells were incubated with 100 μM Cu-Phen, either in the absence (−) or presence (+) of 1 mM carbachol (CCh) (**a, c**). The cross-linking data shown in panel (**b**) were obtained in the absence of carbachol. Note that GTPγS (100 μM) treatment greatly reduced the intensities of the observed cross-linking signals, while atropine (10 μM), an inverse muscarinic agonist, had no effect on the efficiency of cross-link formation (**b**). Western blotting studies were carried out under non-reducing conditions. The antibodies used are indicated underneath the blots. The blots shown are representative of two to four independent experiments. The bands corresponding to cross-linked receptor/$G\alpha_q$ complexes are indicated by arrows.

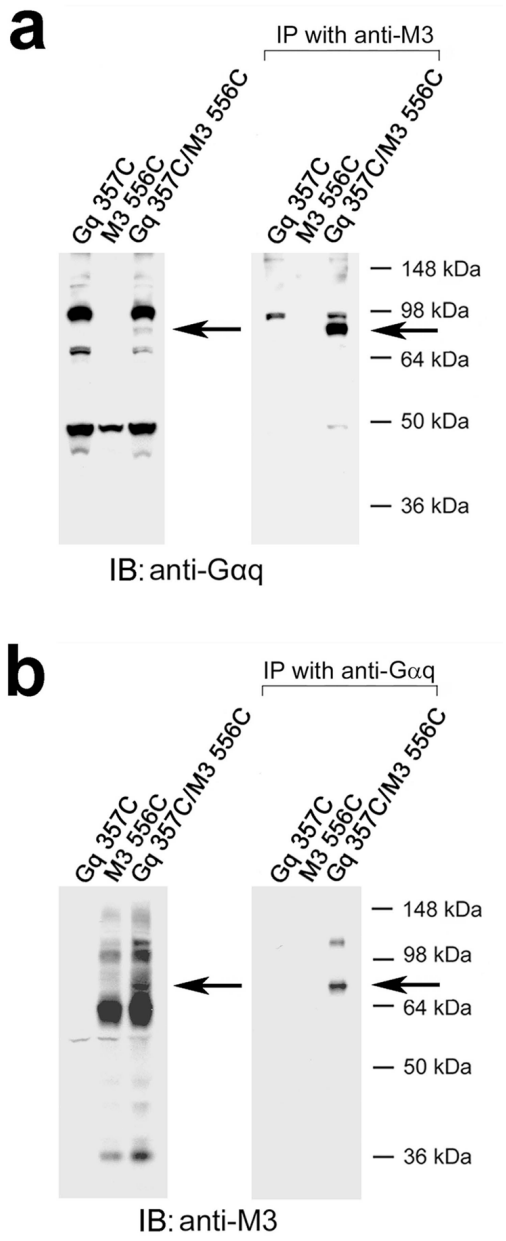

Figure 3.

Co-immunoprecipitation experiments confirming the identity of a representative $G\alpha_q$/M3R complex. (**a, b**) Co-immunoprecipitation of the N357C-$G\alpha_q$/T556C-M3R complex. Co-immunoprecipitation studies were carried out with lysates prepared from COS-7 cells co-expressing the N357C-$G\alpha_q$/T556C-M3R combination. For control purposes, COS-7 cells were also transfected with N357C $G\alpha_q$ or T556C M3R alone. To induce cross-link formation, membrane proteins were incubated with 100 μM Cu-Phen. Following membrane lysis, M3R-containing proteins were immunoprecipitated with a polyclonal anti-M3 antibody, followed by Western blotting studies using an anti-$G\alpha_q$ monoclonal antibody **(a)**. In a reciprocal fashion, $G\alpha_q$-containing proteins were immunoprecipitated with the anti-$G\alpha_q$ antibody, followed by immunoblotting studies using the anti-M3R antibody **(b)**. Co-immunoprecipitation experiments were carried out as described under Supplementary

Methods. The panels to the left show Western blots of samples prior to immunoprecipitation. In all co-immunoprecipitation experiments, the ~80 kDa band was the only immunoreactive species that was consistently detectable by both the anti-M3 and anti-$G\alpha_q$ antibodies. The blots shown are representative of two independent experiments. The bands corresponding to cross-linked receptor/$G\alpha_q$ complexes are indicated by arrows.

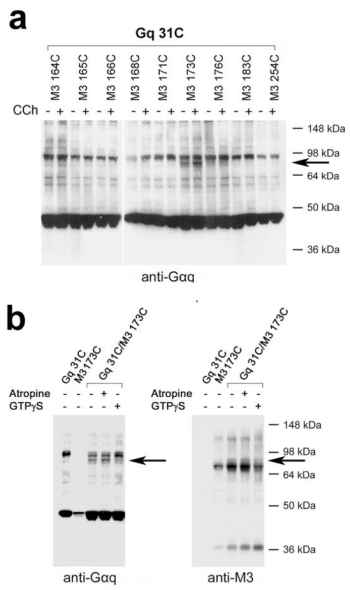

Figure 4.

Cross-link formation between a Cys residue introduced into the αN helix of $G\alpha_q$ (R31C) and a Cys residue substituted into the i2 loop of the M3R (L173C). (**a**) Cross-link formation between R31C $G\alpha_q$ and the L173C mutant M3R. (**b**) Effect of atropine and GTPγS treatment on the formation of the $G\alpha_q$-R31C/M3R-L173C complex. While GTPγS (100 μM) treatment greatly reduced the intensity of the observed cross-linking signal, atropine (10 μM), an inverse muscarinic agonist, had no effect on the efficiency of $G\alpha_q$-R31C/M3R-L173C complex formation. Membranes prepared from transfected COS-7 cells were incubated with 100 μM Cu-Phen in the absence (−) or presence (+) of 1 mM carbachol (CCh). The cross-linking data shown in panel (**b**) were obtained in the absence of carbachol. Western blotting studies were carried out under non-reducing conditions. The antibodies used are indicated underneath the blots. The blots shown are representative of three independent experiments. The bands corresponding to cross-linked receptor/$G\alpha_q$ complexes are indicated by arrows.

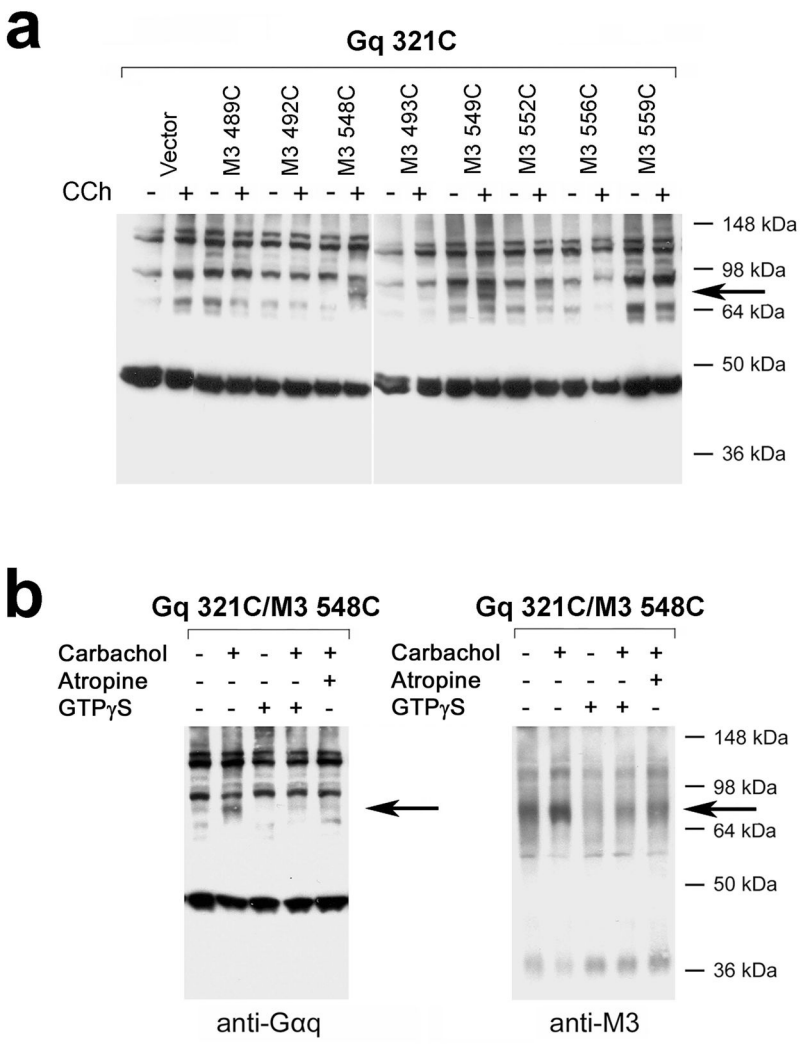

Figure 5.

Agonist-induced cross-link formation between a Cys residue introduced into the α4/β6 loop of $G\alpha_q$ (D321C) and Cys residues substituted into the N-terminal segment of H8 of the M3R. (**a**) Agonist-dependent cross-link formation between the D321C $G\alpha_q$ subunit and the K548C, T549C, and T552C mutant M3Rs. **(b**) Effect of atropine and GTPγS treatment on the formation of the $G\alpha_q$-D321C/M3R-K548C complex. Note that treatment with either GTPγS (100 μM) or atropine (10 μM) prevented the increase in carbachol-induced cross-link formation. Membranes prepared from transfected COS-7 cells were incubated with 0.5 mM BMOE in the absence (−) or presence (+) of 1 mM carbachol (CCh). Western blots were probed with a monoclonal anti-$G\alpha_q$ antibody (**a**) or with both anti-$G\alpha_q$ and anti-M3R antibodies (**b**). The blots shown are representative of three independent experiments. The bands corresponding to cross-linked receptor/$G\alpha_q$ complexes are indicated by arrows.

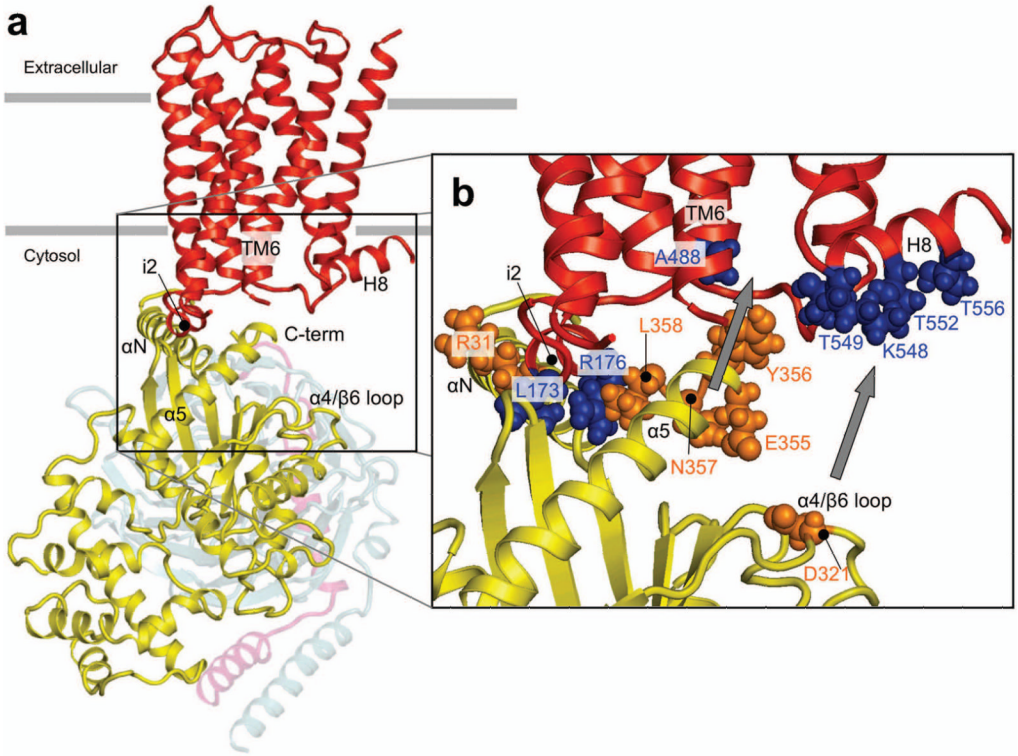

Figure 6.

Molecular model of the M3R/G_q complex. (**a**) Side view of the complex between the inactive state of the M3R and the G_q heterotrimer. The M3R is shown in red, $G\alpha_q$ in yellow, Gβ in grey, and Gγ in pink. **(b)** Enlargement of the M3R/$G\alpha_q$ interface. M3R residues are shown in blue, $G\alpha_q$ residues in orange. The structure shown represents the complex between the resting state of the M3R in contact with the G_q heterotrimer (for details, see Supplementary Methods). The interaction between R31C in the αN helix of $G\alpha_q$ and L173C in the i2 loop of the M3R provided a key contact site for the docking process. The C-terminus of $G\alpha_q$ points toward the intracellular core of the receptor, between the i2 loop and H8. The finding that the C-terminal residues of $G\alpha_q$ can interact with multiple M3R residues in the i2 loop (L173 and R176) and the N-terminal portion of H8 (T549, T552 and T556) suggests that the extreme C-terminus of $G\alpha_q$ is conformationally highly flexible. Agonist-induced M3R activation promoted the formation of cross-links between the extreme C-terminus of $G\alpha_q$ and the cytoplasmic end of TM6 (A488C) (grey arrow) and the N-terminal segment of H8 (T549C and T552C) of the M3R. Moreover, in the activated state of the receptor, a residue in the α4/β6 loop of $G\alpha_q$ (D321C) could be cross-linked to the N-terminal portion of H8 (K548C, T549C, and T552C) (grey arrow). The potential functional implications of theses structural changes are discussed in the text.